100 YEARS Journal of Ecology

British Ecological Society

Journal of Ecology doi: 10.1111/1365-2745.12546

Increasing plant species diversity and extreme species turnover accompany declining soil fertility along a long-term chronosequence in a biodiversity hotspot

Graham Zemunik[1,2]*, Benjamin L. Turner[1,2], Hans Lambers[1] and Etienne Laliberté[1,3]

[1]School of Plant Biology, The University of Western Australia, Crawley (Perth), WA 6009, Australia; [2]Smithsonian Tropical Research Institute, Apartado 0843-03092, Balboa, Ancon, Panama; and [3]Département de Sciences Biologiques, Institut de Recherche en Biologie Végétale, Université de Montréal, 4101 Sherbrooke Est, Montréal, QC H1X 2B1, Canada

Summary

1. Long-term soil chronosequences provide natural soil fertility gradients that can be used to explore linkages between soils and plant community composition and diversity. Well-studied forested soil chronosequences have revealed that local (α) plant diversity increases with greater soil age and declining fertility, but corresponding changes in species turnover and beta (β) diversity have not been explored, particularly in extremely species-rich regions.

2. We quantified changes in plant species diversity and community composition, and identified the edaphic drivers of these changes, along a >2-million year retrogressive dune chronosequence in the south-west Australia biodiversity hotspot.

3. We found greater plant species diversity across all growth forms as soil development proceeded and concentrations of soil nutrients, particularly phosphorus (P), diminished to extremely low levels (surface soil total P concentrations of 6 mg P kg^{-1}). Despite the high plant α diversity on older nutrient-impoverished soils, species turnover across the chronosequence was exceptionally high when all growth forms were considered (mean of 1% of species shared between the youngest and oldest soils), and there was complete turnover of woody species along the chronosequence. Such extreme species turnover across the chronosequence reflected large changes in soil chemical properties. In addition, β diversity within individual chronosequence stages increased with declining soil fertility. Shrubs remained the dominant and most speciose growth form throughout the chronosequence.

4. *Synthesis*. The large increase in plant α diversity and the extreme species turnover associated with declining soil fertility highlight the central role of soil properties in driving plant community assembly during long-term ecosystem development, previously only reported from comparatively species-poor regions. Our finding that plant β diversity increased with declining soil fertility points to a novel mechanism whereby extremely low soil fertility, rather than high productivity, promotes high β diversity. These results suggest that the interaction of an exceptionally diverse plant species pool and nutrient-impoverished soils provides the basis for the maintenance of such high β diversity at extremely low soil fertility.

Key-words: beta diversity, determinants of plant community diversity and structure, ecosystem development, non-mycorrhizal plant species, nutrient-impoverished soil, pedogenesis, phosphorus, retrogression, species richness

Introduction

Primary succession is associated with the initial stages of soil and ecosystem development and results in an increase in plant species diversity as plants gradually colonize a site (Odum 1969; Grime 2001). Many of the early successional species (i.e. 'ruderal' species sensu Grime 2001) that colonize recently exposed substrates grow quickly, are short-lived and rapidly produce many, readily dispersed seeds, making these early stages of succession amenable to study (Connell & Slatyer 1977). Direct observational studies of soil and ecosystem development in the longer term, however, are impossible

*Correspondence author: E-mail: graham@graduate.uwa.edu.au

given that soil-forming processes operate over hundreds to many thousands of years. For this reason, long-term soil chronosequences are recognized as invaluable model systems for the study of long-term ecosystem development and the response of plant species diversity to pedogenic change (Vitousek 2004; Peltzer *et al.* 2010; Walker *et al.* 2010; Laliberté *et al.* 2013).

Soil chronosequences are space-for-time substitutions, comprising series of soils derived from the same parent material but with differing periods of soil formation (Jenny 1946; Stevens & Walker 1970). Studies using soil chronosequences have shown that long-term soil development results in characteristic shifts in soil properties, including declining pH and phosphorus (P) concentrations, and corresponding shifts in plant communities and plant species diversity (Walker & Syers 1976; Crews *et al.* 1995; Richardson *et al.* 2004; Wardle *et al.* 2008; Laliberté *et al.* 2012). Although a small number of well-studied long-term chronosequences (e.g. Thompson 1981; Crews *et al.* 1995; Richardson *et al.* 2004; Wardle *et al.* 2008; Gundale *et al.* 2011) have provided valuable insights into the responses of forested ecosystems to long-term soil development, shrubs and herbs, by contrast, are minor components of these chronosequences in terms of standing biomass. However, some of the most species-rich regions are shrub-dominated communities in seasonally dry climates (Cowling *et al.* 1996; Hopper & Gioia 2004), and the pattern emerging from chronosequence studies is that the species richness of shrubs and herbs, unlike that of trees, generally increases with ecosystem retrogression – the reduction of many ecosystem processes as soils age (Wardle *et al.* 2008; Laliberté *et al.* 2013).

The Jurien Bay dune chronosequence (Laliberté *et al.* 2012; Laliberté, Zemunik & Turner 2014) is a species-rich chronosequence located within the south-west Australian global biodiversity hotspot (Myers *et al.* 2000) and is dominated by shrubs throughout. Laliberté, Zemunik & Turner (2014), using the Jurien Bay chronosequence as a model system to determine the factors that best explain variation in local plant species richness along resource gradients, found that environmental filtering from the regional flora, not various aspects of local soil resource availability, most strongly determined the local species diversity. However, the details of the shifts in plant diversity and community composition along the sequence have not previously been described, and these are the focus of the present study. Furthermore, other processes, such as stochastic priority effects (e.g. Chase 2010), may affect beta (β) diversity (i.e. variation in community composition across sites), which was not explored by Laliberté, Zemunik & Turner (2014). Chronosequences, as strong fertility and productivity gradients, also allow tests of hypotheses linking β diversity to increasing resource availability or productivity (Chase & Leibold 2002; Harrison *et al.* 2006). These hypotheses have not yet been evaluated for plants along natural, strong and well-defined resource availability gradients such as those provided by soil chronosequences (but see Martínez-García *et al.* 2015, for arbuscular mycorrhizal fungi).

In this study, we characterized plant communities along the Jurien Bay dune chronosequence and analysed the soils for nutrients and other chemical properties to further our understanding of how soil development has affected the system's plant diversity, species turnover and its progression into retrogression. Recent work in the system (Laliberté, Zemunik & Turner 2014) led us to expect an increase in species richness and diversity across the chronosequence, consistent with the synthesis by Wardle *et al.* (2008), who found an increase in the richness of all vascular species along a series of contrasting long-term soil chronosequences with retrogressive phases. The large regional species pool with many species adapted to acidic soils (Laliberté, Zemunik & Turner 2014) led us to hypothesize that β diversity and species turnover within each chronosequence stage would increase with declining soil fertility and decreasing soil pH, and that there would be high plant species turnover across the entire chronosequence. Although recent advances linking β diversity to productivity have stressed the scale-dependent nature of β diversity, our study within a single region allowed us to test the effect that soil development and associated changes in soil resource availability and productivity (Laliberté *et al.* 2012; Turner & Laliberté 2015) have on β diversity, without the confounding factors often introduced when comparing widespread regions with different regional floras.

Materials and methods

SITE SELECTION

The Jurien Bay dune chronosequence (30°01′ to 30°24′ S; 114°58′ to 115 11′ E; ~45 km N to S; and ~15 km W to E) consists of three main dune systems: the Quindalup, Spearwood and Bassendean dunes, corresponding to sea-level highstands during the Holocene (Quindalup dunes), the Middle Pleistocene (Spearwood dunes) and the Early Pleistocene (Bassendean dunes) (McArthur 2004; Laliberté *et al.* 2012; Turner & Laliberté 2015). Climate, vegetation and soils have been described elsewhere (Laliberté *et al.* 2012; Hayes *et al.* 2014; Laliberté, Zemunik & Turner 2014; Turner & Laliberté 2015). The study used a randomized stratified sampling design, with the three main dune systems delineated into six chronosequence stages (Laliberté, Zemunik & Turner 2014; Zemunik *et al.* 2015). The Quindalup dune system comprises stages 1–3: (1) recently stabilized dune sand; (2) well-developed soil further inland supporting mature vegetation; and (3) well-developed soil of dunes within approximately 1 km west of the Quindalup–Spearwood transition. The Spearwood dunes contain two stages (4 and 5), differentiated by the degree of soil development: (4) dunes closest to the coast, with sandy soil overlying limestone, generally within 1 m of the soil surface; (5) fully decalcified Spearwood sand, at least several metres deep. The Bassendean dunes comprise stage 6 and were not further delineated due to the absence of consistent topographic or soil features allowing a clear distinction to be made within the system.

STUDY PLOTS

Vegetation sampling was described in detail elsewhere (Laliberté, Zemunik & Turner 2014; Zemunik *et al.* 2015). Briefly, plot locations within stratified regions were randomly generated as points in a

geographic information system model (Quantum GIS Development Team, 2012); each point represented the centre of a 10 × 10 m plot. Ten plots were located within each of the six stages, giving a total of 60 plots for the entire dune chronosequence (Fig. S1, Supporting Information; Table S1). The mean distance between neighbouring plots was 2.1 km; we deemed this plot separation sufficient to minimize the effects of spatial autocorrelation between plots.

To estimate canopy cover and abundance within the 10 × 10 m plots, seven randomly positioned 2 × 2 m subplots were surveyed within each plot. Seven subplots were assessed as giving an accurate representation of community composition and diversity within the 10 × 10 m plot area by calculating species accumulation curves with nonparametric estimators using the ESTIMATES software package (Colwell 2013), with data from a particularly species-rich plot from stage 6 (oldest soils). The 28% plot coverage given by the seven subplots fell near the upper end of a range recommended in a prior study in similar species-rich shrublands from this region (Chiarucci *et al.* 2003).

FLORA SURVEYS

Surveys of all vascular plants in the plots were done in August, September, October and November of 2011, and January, February, March and September of 2012. Plots that were initially surveyed outside the peak flowering season (approximately August to November) were resurveyed in September 2012 to ensure that seasonal (i.e. annual or geophytic) species would be included. The observed vascular plants rooted within each 10 × 10 m plot were recorded and identified to the species (or subspecies) level. Within each subplot, the number of individuals was counted for species whose stems were either fully or partially within the subplot, and their median height and width were also recorded. Canopy cover was visually estimated for all species with vegetation cover within the subplot, irrespective of the location of their stem, as a percentage of the subplot covered by a vertical projection of the canopy. Consistency of visual estimation was maintained by the estimation being done by the same person (G. Zemunik) throughout all surveys. Species known to be clonal were classified as separate individuals if stems or culms were >20 cm from others belonging to the same species.

SOIL ANALYSES

Soil analyses were described in detail by Turner & Laliberté (2015). In brief, soil samples were taken at 0–20 cm depth from each 2 × 2 m subplot in June 2012, giving a total of 420 soil samples (seven samples from each of the 60 plots). From these subplot samples, soil pH (in water and 10 mM $CaCl_2$), total soil carbon (C) and nitrogen (N) were determined by automated combustion, and dissolved organic N (DON) by KCl extraction. We determined exchangeable cations (aluminium, calcium (Ca), iron (Fe), potassium (K), magnesium (Mg), manganese (Mn) and sodium (Na)) by extraction in 0.1 M $BaCl_2$ and detection by inductively coupled plasma optical emission spectrometry (ICP-OES) on an Optima 7300 DV (Perkin Elmer, Inc, Shelton, CT, USA). Key micronutrients (copper, Fe, Mn and zinc) were extracted in Mehlich-III solution (Mehlich 1984) with detection by ICP-OES. Bulked subplot soil samples were used to determine plot-level readily exchangeable P by extraction with anion-exchange membranes (resin P), and total soil Ca, K, Mg, Mn and P by digestion in concentrated nitric acid and detection by ICP-OES. Carbonate concentrations of the bulked soil samples were determined by mass loss after addition of 3 M HCl.

DATA ANALYSES

All data analyses used R (R Development Core Team, 2013) with the specific packages as stated below. Rarefaction, based on the minimum number of individual plants recorded across all 60 plots, was performed with the 'rarefy' function in the 'vegan' package (Oksanen *et al.* 2013). Confidence intervals were calculated by the 'effects' package using generalized least squares models as implemented by the 'nlme' package (Pinheiro *et al.* 2015), with appropriate variance functions chosen to minimize heteroscedasticity of the residuals. Letters used to denote different groups, based on the Tukey HSD test, were generated by the 'lsmeans' package (Lenth 2014).

Diversity and evenness values were calculated using the 'diversity' function in the vegan package. Species richness at the chronosequence stage level was estimated with the 'specpool' function from vegan, using the Chao (1984) and second-order Jackknife estimators; in another kwongan vegetation system, the second-order Jackknife estimator has been shown to approach 'true' species richness most quickly (Chiarucci *et al.* 2003). For the purpose of richness estimation, species that had cover in the subplot were counted as present (assigned a minimum count of one) even if there were no individuals of that species rooted in the subplot. To further explore the compositional change of species in differing plots, we quantified the percentage of species shared between pairs of plots, both within and between chronosequence stages. This analysis was done with the vegan 'vegdist' function using Jaccard similarity (i.e. 1 – dissimilarity) on the presence/absence data.

Unconstrained ordination of plots (sites) was performed by nonmetric multidimensional scaling (NMDS) using the vegan 'metaMDS' function. Bray–Curtis dissimilarity values, calculated on untransformed relative cover data by the 'vegdist' function from the vegan package, were used in the NMDS; other dissimilarity methods were also tested and yielded qualitatively similar results. To increase the chance of finding a global minimum in the NMDS procedure, the 'metaMDA' function was executed twice, with the best result of the first being passed to the second instance. Only the results from ordination in two dimensions are presented, as these ordinations produced sufficiently low stress values and are easier to interpret. PERMANOVA post hoc tests using Bray–Curtis dissimilarity with 10^4 permutations were performed with the vegan 'adonis' function. Pairwise comparisons on the dissimilarity between each pair of chronosequence stages also used the 'adonis' function, with adjustments for multiple comparisons using the 'p.adjust' function with the 'holm' method (Holm 1979). Multivariate dispersions (Anderson 2006) of the plots (i.e. beta diversity), for all species and woody species only, were calculated using the vegan 'betadisper' function and the Bray–Curtis, Kulczynski, Hellinger and Jaccard dissimilarity indices. The multivariate dispersion calculated with the Jaccard dissimilarity index used the presence/absence data; all other dissimilarity calculations used untransformed relative cover values. Significance testing of the plot groupings was done with the vegan 'permutest' function, using 999 permutations.

Constrained ordination was done using canonical redundancy analysis (RDA) (Borcard, Gillet & Legendre 2011), implemented by the 'decostand' and 'rda' functions from the vegan package. The RDA used both relative cover and abundance data (both Hellinger-transformed) as the response variable (Legendre & Gallagher 2001), and a minimal set of soil elemental concentrations and properties as the explanatory variables. To obtain the minimal explanatory set of soil variables, a forward selection procedure was used, implemented by the 'forward.sel' function from the 'packfor' package (Dray, Legendre & Blanchet 2013); the variables selected were additionally verified by

a second forward selection procedure, using the vegan 'ordistep' function. The initial set of soil variables included only the exchangeable cations, when both total and exchangeable were available, due to their presumed greater bioavailability, although total and exchangeable values were well correlated. From that set of variables, those with concentrations deemed too low to be physiologically relevant (e.g. exchangeable Na) were also excluded from the initial selection. Variance inflation factors (Borcard, Gillet & Legendre 2011) were calculated on the variables from the RDA using the vegan 'vif.cca' function to identify whether any of the selected variables were redundant; all selected variables had variance inflation factors well below the recommended threshold of 10. Permutation testing of the RDA model was done using the vegan 'permutest' function with 99 999 permutations.

To obtain additional insights into the environmental drivers of plot similarities and groups and to help classify the plant communities into distinct, plausible groups, multivariate regression trees (MRT) were constructed using the untransformed relative cover of plant species as the response and, as the explanatory variables, a wide range of soil variables with physiologically meaningful concentrations: total P, pH ($CaCl_2$), resin P, exchangeable Mg, organic C, total and exchangeable Ca, Fe (Mehlich-III), copper (Mehlich-III), Mn (Mehlich-III), zinc (Mehlich-III), exchangeable K and dissolved organic N. Each MRT was calculated using the 'mvpart' function from the 'mvpart' package (De'ath 2014), with 150 multiple cross validations. Several alternative trees were produced by varying the number of leaf nodes, whilst ensuring that the cross-validated relative error (CVRE) was within the recommended guideline of within one standard error of the minimum CVRE (De'ath 2002). Because some splits in the decision trees were only marginally better (in terms of the variance explained) than other possible splits, we also tested the sensitivity of the results to small changes in the variables by the addition of small scaling factors to the variables. This was also deemed necessary as the MRT algorithm splits the tree based on the relative error (variance explained), which may make the tree susceptible to overfitting of the data; by contrast, the CVRE counters against this overfitting, and hence predictive accuracy is viewed as being better estimated from the CVRE (De'ath 2002). Dendrogram groupings for the MRT were generated by the 'dendro_data' function from the 'ggdendro' package (de Vries & Ripley 2013). Indicator species – species that best represent each group – for the MRT groups were calculated with the 'multipatt' function from the 'indicspecies' package (De Cáceres & Legendre 2009), using the indicator statistic 'IndVal.g', as proposed by De Cáceres, Legendre & Moretti (2010). This indicator statistic, applicable to each species in a group and bounded by 0 and 1, is related to two probabilities, *P(A)* and *P(B)*, by the formula $\sqrt{P(A)} \times P(B)$, where *P(A)* denotes the probability of the plot being in the group, given the presence of that species in the plot, and *P(B)* is the probability of finding that species in a plot within the group.

Results

ALPHA DIVERSITY INCREASES WITH SOIL AGE

Plant species density and rarefied richness increased markedly with increasing soil age across the chronosequence (Fig. 1). In terms of plant growth forms, the increase in species density was greatest for perennial species (Fig. 1a). Conversely, annual species were a larger component of the community in the younger stages, although never comprising more than a mean of 37% of the species and 7% of the relative cover (in stage 2). Whilst rarefied species richness increased some 250% across the sequence, the mean observed α diversity increased threefold and the effective or 'true' (sensu Tuomisto 2010) α diversity increased 3.5 times (Table 1).

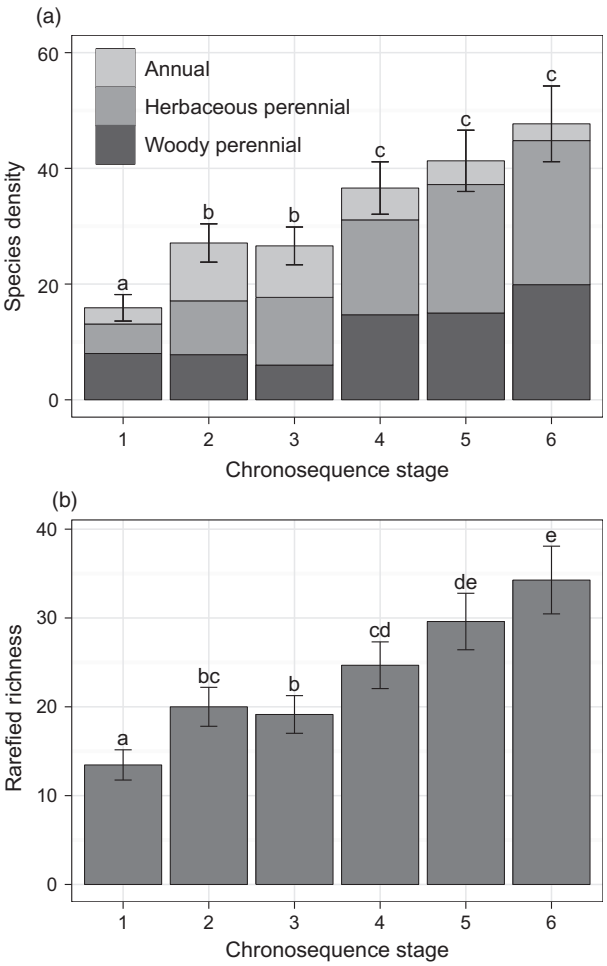

Fig. 1. Plant species density (species per 28 m^2) for the main plant growth forms (a) and the mean richness rarefied by the minimum of individuals for all species and growth forms (b) across the Jurien Bay chronosequence. Error bars represent 95% confidence intervals. Letters above each mean represent Tukey HSD groupings ($P \leq 0.05$).

Commonly used metrics of α diversity, the Simpson (1/D) and Shannon diversity, also increased across the sequence (Fig. 2); the Simpson diversity increased more than three times. Species evenness did not decline; rather, the Shannon, or Pielou, evenness exhibited significantly higher evenness in the final stage in comparison with that in the first (Fig. 2d).

HIGHEST BETA DIVERSITY IN THE OLDEST SOILS

Traditional measures of β diversity (multiplicative and additive β diversity) increased with increasing soil age (Table 1), but as β diversity can be defined to measure different aspects of species compositional change, the different measures that were used performed differently. The greatest increase in β diversity was with the additive β diversity measure, as would be expected, given that γ diversity increased substantially

Table 1. Observed and estimated alpha (α) and gamma (γ) richness, and calculated beta (β) diversity. Symbols: γ, observed richness or gamma diversity; $^1D_\gamma$, true gamma diversity (sensu Tuomisto 2010); Chao, Chao 1 species richness estimator; Jack 2, Jackknife 2 species richness estimator; $\overline{\alpha}$, mean observed alpha diversity; $\overline{\alpha}_{Rarefied}$, mean alpha diversity, rarefied to the minimum number of individuals; $^1D_\alpha$, true alpha diversity (sensu Tuomisto 2010), or effective diversity; $\beta_{\gamma/\alpha}$, multiplicative β diversity; $\beta_{\gamma-\alpha}$, additive β diversity; $^1D_\beta$, 'true' β diversity (sensu Tuomisto 2010)

	Gamma				Alpha			Beta		
Stage	γ	$^1D_\gamma$	Chao	Jack 2	$\overline{\alpha}$	$\overline{\alpha}_{Rarefied}$	$^1D_\alpha$	$\beta_{\gamma/\alpha}$	$\beta_{\gamma-\alpha}$	$^1D_\beta$
1	48	16.9	81	78	15.9	13.4	6.8	3.01	32.1	2.47
2	75	24.6	89	100	27.1	19.8	12.1	2.77	47.9	2.03
3	75	16.7	123	121	26.6	19.1	11.2	2.82	48.4	1.49
4	122	27.5	194	196	36.6	24.4	12.7	3.33	85.4	2.15
5	135	34.5	213	221	41.3	29.1	18.2	3.27	93.7	1.89
6	176	63.9	265	286	47.7	33.7	23.9	3.69	128.3	2.67

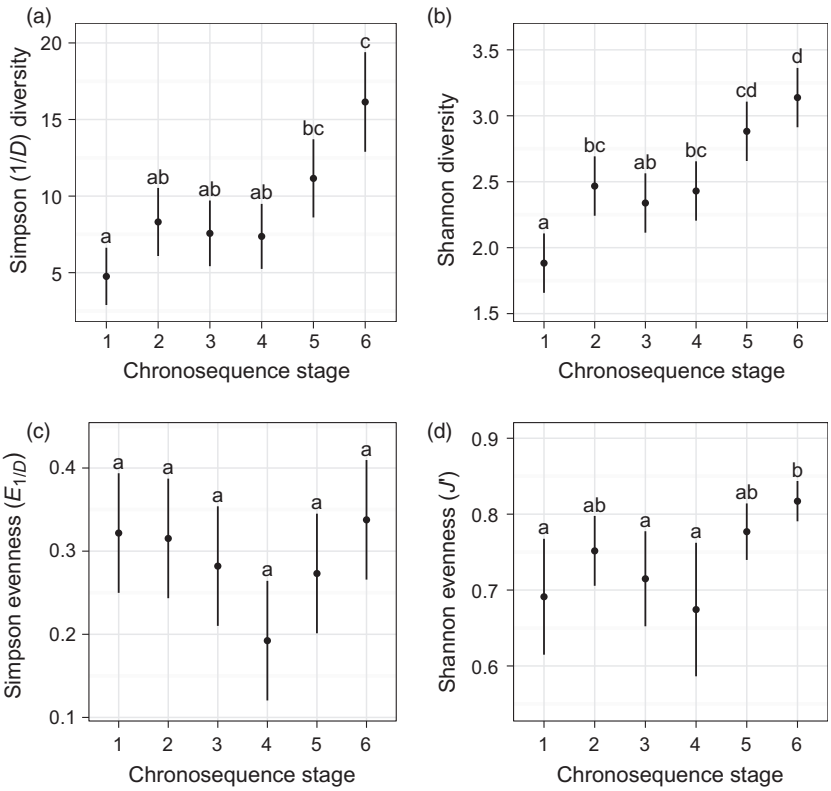

Fig. 2. Simpson (1/D) (a) and Shannon diversity (b), along with Simpson (c) and Shannon (Pielou) eveness (d) for plant species across the chronosequence. Error bars represent 95% confidence intervals. Letters above each bar represent Tukey HSD groupings ($P \leq 0.05$).

(Table 1; see also Laliberté, Zemunik & Turner 2014). By contrast, the smallest increase in β diversity with increasing soil age and declining soil fertility was in the 'true' β diversity of Tuomisto (2010), with all intermediate stages having lower β diversities than the first and last. Beta (multivariate) dispersion of the plots within each chronosequence stage did not show significant differences in the degree of dispersion within each stage, when considering all species. However, the multivariate dispersion of plots when considering only woody species was more distinct and marginally significant (e.g. $P = 0.08$, Bray–Curtis dissimilarity, Table S5), with chronosequence stages 2 and 3 being less dispersed than all others. Multivariate dispersions for woody species, calculated using two other dissimilarity indices (Kulczynski and Hellinger), resulted in a slightly greater distinction between plot groupings, and correspondingly lower *P*-values (Table S5); again, chronosequence stages 2 and 3 had the lowest multivariate dispersions, and stages 1 and 6 had the consistently greatest multivariate dispersions. By contrast, multivariate dispersion values for all species were broadly unchanged when calculated using the other dissimilarity indices (Table S5).

GAMMA DIVERSITY INCREASES WITH INCREASING SOIL AGE

Gamma (γ) diversity increased markedly with increasing soil age, with the increase in γ diversity from the youngest to

oldest soils (about 3.7 times) generally exceeding that for α diversity (Table 1). The Chao 1 and second-order Jackknife estimators of γ diversity also increased by about the same amount as the observed γ diversity. There was no consistent relationship between the number (or density) of individual plants per plot and the chronosequence stage, and hence the diversity, for all plants, perennial plants as well as woody plants (Fig. S3).

HIGH SPECIES TURNOVER ACROSS THE CHRONOSEQUENCE

Non-metric multidimensional scaling (NMDS) of the relative cover of plots (sites) produced groupings of plots consistent with each chronosequence stage for all species (Fig. 3) and for species of woody growth forms (Fig. S4). Successive stages were more similar than non-adjacent stages, and there was a gradual, directional shift in community composition from one chronosequence stage to the next (indicated by the arrow in Fig. 3), with stages 2 and 3 dominated by *Melaleuca systena* Craven (Myrtaceae) and the older soils dominated by *Banksia* species (Proteaceae) (Table S2). PERMANOVA tests gave support for these site groups ($P \leq 10^{-4}$, Pseudo-$F = 10.16$, $R^2 = 0.48$), and *post hoc* tests between all pairs of stages were significantly different, except for the plots in stages 2 and 3 ($P = 0.13$).

The percentage of species shared between pairs of plots decreased with each chronosequence stage, both when considering all species (Fig. 4a) or only woody species (Fig. 4b). The greatest percentage of shared species (mean of 41%) was between pairs of plots in the oldest Quindalup stage (stage 3), whilst in the final chronosequence stage (Bassendean), a mean of only 28% of species were shared between pairs of plots. Very few species (1 to 15%) were shared between the Quindalup dune stages (stages 1–3) and the older stages (4–6), and even fewer (0–9%) when only woody species were considered; in fact, no woody species at all were shared between pairs of plots from the first and last chronosequence stages (i.e. there was complete woody plant species turnover). The only species found throughout the chronosequence were the annual herbs, *Trachymene pilosa* Sm. (Araliaceae) and *Crassula colorata* var. *acuminata* (Reader) Toelken (Crassulaceae); the semi-annual herb, *Opercularia vaginata* Juss. (Rubiaceae), the geophyte *Thysanotus patersonii* R.Br. (Asparagaceae), and the southern rush, *Desmocladus asper* (Nees) B.G.Briggs & L.A.S.Johnson (Restionaceae). No species of woody plants extended throughout all stages of the chronosequence, although the N-fixing legume *Acacia rostellifera* Benth., and the myrtaceous *Melaleuca systena* were found in five out of the six stages; both of these species were absent in the Bassendean dunes (stage 6).

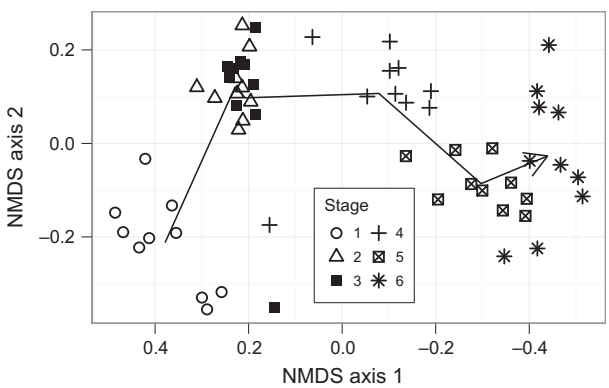

Fig. 3. Non-metric multidimensional scaling biplot (NMDS) with the directionality of the chronosequence (stage 1–6) represented by the arrow. Bray–Curtis dissimilarity using all species was used in the NMDS; plot stress: 0.14.

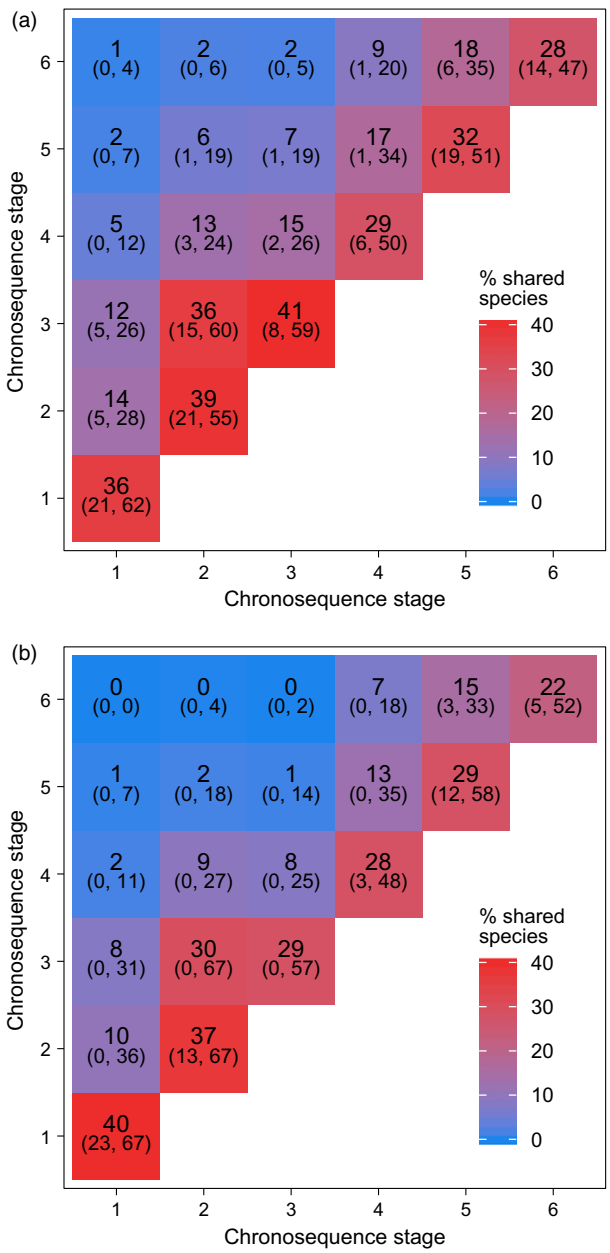

Fig. 4. Mean percentage of plant species shared between pairs of plots (i.e. Jaccard dissimilarity) within each chronosequence stage, for (a) all species and (b) woody species only. The range is shown in brackets.

SHIFTS IN COMMUNITY COMPOSITION LINKED TO CHANGES IN SOIL PROPERTIES

Selection of variables for canonical redundancy analysis (RDA) was by two different forward selection procedures; both yielded the same set of five soil variables: pH, DON, Mehlich-III-Fe, mean carbonate and exchangeable K (Fig. 5). Several variables that would be expected to be important factors (soil total P and N) were not selected, due to strong correlation with the selected variables. For example, total soil P (or, more precisely, the logarithm of total soil P) was strongly correlated with soil pH (r = 0.97). The variance inflation factors, which give a measure of the collinearity of each variable with other variables, were low (all factors < 5.8). Site groupings by the RDA analysis produced a clustering of sites similar to the NMDS ordination, with sites aligned closely to the chronosequence stage. The grouping of Quindalup (stages 1–3) sites was explained by relatively high soil pH and carbonate concentrations, with only stages 2 and 3 having high DON and exchangeable K concentrations. Changes in composition of sites in stages 4–6 were explained by low concentrations of all selected variables, except Fe. Canonical redundancy analysis using abundance, rather than relative cover data, produced similar site groupings (Fig. S5).

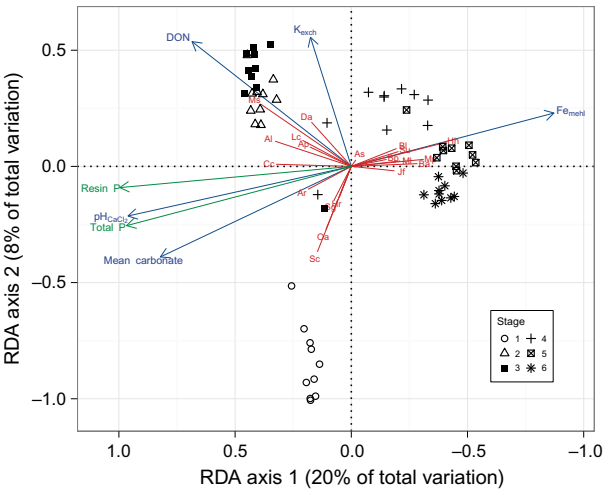

Fig. 5. Canonical redundancy analysis (RDA) of the plant species (Hellinger-transformed) cover data, as explained by soil variables (R^2 = 0.38; adjusted R^2 = 0.32; $P \leq 10^{-5}$). The soil variables shown (blue) are the minimal set of variables that were included in the model using a forward selection procedure, with the supplementary soil variables (green) included to illustrate the high correlation between soil pH and soil P concentrations. Only the five most abundant species (by cover) in each chronosequence stage are shown (red) by two-letter codes: (*Acacia lasiocarpa*, Al; *Acacia rostellifera*, Ar; *Acacia spathulifolia*, As; *Acanthocarpus preissii*, Ap; *Banksia attenuata*, Ba; *Banksia leptophylla* var. *melletica*, Bl; *Banksia prionotes*, Bp; *Conostylis candicans* subsp. *calcicola*, Cc; *Desmocladus asper*, Da; *Hibbertia hypericoides*, Hh; *Hibbertia racemosa*, Hr; *Jacksonia floribunda*, Jf; *Lepidosperma calcicola*, Lc; *Melaleuca leuropoma*, Ml; *Melaleuca systena*, Ms; *Mesomelaena pseudostygia*, Mp; *Olearia axillaris*, Oa; *Scaevola crassifolia*, Sc; *Scholtzia umbellifera*, Su; *Spyridium globulosum*, Sg). The first two canonical axes represent 28% of the total variation in community structure and 74% of the environmentally structured variation (i.e. the variation explained by the soil variables).

CLASSIFICATION OF PLANT COMMUNITIES AND INDICATOR SPECIES

The most informative and plausible groupings of sites by the multivariate regression tree (MRT) procedure was with the generation of a tree with seven leaf nodes. Although the absolute lowest R^2 value was produced using soil variables without any scaling factors (Fig. S6), the tree with the best cross-validated relative error (0.48) used scaling factors of 1.04 for the variables DON and exchangeable calcium (Fig. 6). Both trees contained common groupings of sites, with the main structural difference resulting from branching beginning with either DON or total P. Because the range of total P (72-fold) far exceeds the range of DON (2.6-fold), we consider the tree rooted with a decision on total P as the most plausible (Fig. 6). The MRT algorithm, which maximizes the predictive power of the tree, resulted in a different set of soil variables from that produced by the RDA, which maximized the explanatory power. The site groups from the MRT showed strong affinity to each chronosequence stage, whilst also isolating some sites with atypical plant community composition for a given chronosequence stage (e.g. Group 2 in Fig. 6). Total soil P separated the great majority of the sites in stages 4–6 from the sites in stages 1–3, with further selections in the decision tree arising from DON, organic carbon, Fe (Mehlich-III) and pH ($CaCl_2$) (Table 2). Indicator species for each MRT group generally had high indicator statistics (Table 3), with the indicator species for groups corresponding to stages 1, 5 and 6 having the highest indicator statistics (the best indicator for those groups ranged from 0.94 to 1.0); two species, *Olearia axillaris* (DC.) Benth. and *Scaevola crassifolia* Labill., were perfect indicators (indicator statistic = 1) for the youngest chronosequence stage (Group 3 in Table 3). Pairs of groups joined by the penultimate nodes of the tree also produced high indicator statistics (ranging from 0.91 to 0.95), and these especially highlighted the affinities between stages 2 and 3 and between stages 5 and 6.

MAJOR FLORISTIC PATTERNS

In total, 347 plant taxa from 57 families were found in the subplots of the chronosequence. By relative cover, the dominant families were the Myrtaceae (mean 18%), Fabaceae (16%) and Proteaceae (14%). However, cover throughout the chronosequence was not uniformly distributed (Fig. S7), with stages 4–6 being dominated by the Proteaceae (28%) and Fabaceae (24%), and the Goodeniaceae having the highest relative cover (19%) in stage 1. Although the relative cover of some plant groups decreased with soil age, by contrast, richness usually increased (Table S4). For example, mean relative cover of the five Goodeniaceae found in the Bassendean stage (6) was <0.5%, but only one species contributed to the cover (mean 19%) in stage 1.

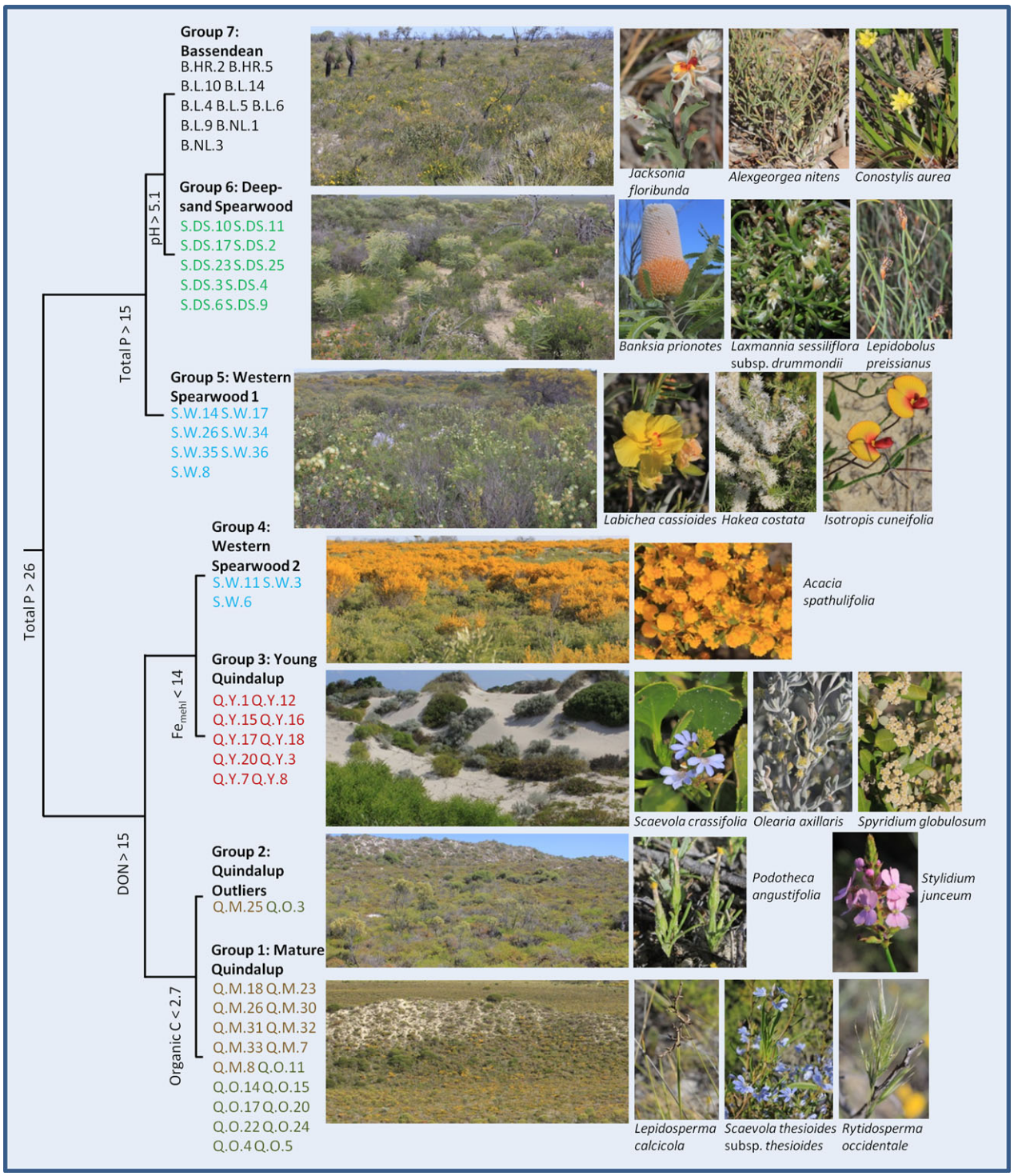

Fig. 6. Multivariate regression tree, which groups sites (separated using Bray–Curtis dissimilarities) based on soil variables. The plot codes (see Fig. S1) are given for each group. Adjacent to the site groupings are representative photos of the vegetation for that group. A selection of indicator species for each group (up to the best three, see Table 3) is shown on the right. The depth of each branch is proportional to the amount of variance explained by that branch. In this tree, a scaling factor of 1.04 was applied to the variables dissolved organic nitrogen (DON) and exchangeable calcium in order to minimize the cross validation relative error (CVRE) and fine-tune the splits. R^2 = 0.73, CVRE = 0.48 (±0.05 SE).

Of the major growth forms, shrubs had a mean relative cover of 55%, sedges 13%, trees 12% and perennial herbs 10% (Fig. S8). The mean canopy height weighted by relative cover was lowest in stages 2 and 3, possibly due to the high abundance of parasitic plants (Lauraceae and Santalaceae in Fig. S7) in combination with a greater distance to the water-table in those dunes; canopy height remained <1 m throughout (Fig. S9a). Shrubs were the dominant growth form, ranging from two to eight times the relative cover of the next most abundant growth form. The relative cover of

Table 2. Values of the soil variables used in the multivariate regression tree (Fig. 6) for each chronosequence stage

Stage	DON (mg N kg^{-1})	Total P (mg^{-1} kg^{-1})	Fe_{mehl} (mg^{-1} kg^{-1})	pH
1	9.2 [8.4, 10.0]	370 [338, 403]	2.7 [1.4, 3.9]	8.2 [8.1, 8.2]
2	23.7 [19.1, 28.5]	436 [409, 463]	1.0 [0.5, 1.5]	7.8 [7.8, 7.9]
3	19.2 [16.3, 22.1]	288 [191, 385]	2.7 [1.8, 3.6]	7.7 [7.7, 7.8]
4	10.2 [7.9, 12.5]	24 [18, 31]	38 [31, 44]	5.9 [5.6, 6.2]
5	9.3 [8.0, 10.6]	9.1 [7.2, 11.0]	39 [32, 45]	5.4 [5.2, 5.6]
6	9.0 [7.9, 10.0]	6.0 [4.0, 8.0]	25 [19, 32]	4.8 [4.6, 5.0]

Mean values with 95% confidence intervals (in square brackets) are shown. The pH was measured in 10 mM $CaCl_2$. DON, dissolved organic nitrogen; P, phosphorus; Fe, iron.

shrubs decreased in stages 2 and 3; the decrease of shrub and tree cover combined was about 47% in stages 2 and 3, but they covered a mean of between 74 and 80% in all other stages. By contrast, cover of perennial herbs, sedges and southern rushes increased in stages 2 and 3: the mean relative cover was about 45% in stages 2 and 3, and between 18 and 24% in all other stages. The absolute canopy cover and amount of bare ground varied little in stages 2 through to 6, although stage 1 had about twice as much bare ground as all other stages (Fig. S9b,c). Shrubs were the most species-rich growth form (Table S3); the number of shrub taxa also increased fourfold. Sedges showed the greatest proportional increase in species richness, with 12 times as many taxa in the last chronosequence stage than in the first.

Discussion

Alpha diversity of the plant community of the Jurien Bay dune chronosequence increased greatly with declining soil fertility, but in contrast to other well-studied forested chronosequences (e.g. Wardle *et al.* 2008), shrubs dominated throughout. Alpha and γ diversity increased markedly with declining soil fertility and, by any measure, β diversity did not decrease (most formulations of the metric showed an increase in β diversity with increasing soil age and declining soil fertility). This is opposite to the hypothesized pattern of increasing β diversity with higher resource availability and primary productivity observed in experimental studies of aquatic life-forms (Chase & Leibold 2002) and empirical studies on a limited number of plant growth forms (Harrison *et al.* 2006). Contrary to previous studies (e.g. Wardle *et al.* 2008), our sampling design allowed us to calculate rarefied α diversity for all growth forms, rather than only tree species; the finding that the rarefied α diversity increased markedly provided additional support for our hypothesis that local plant species diversity would increase with increasing soil age and declining soil fertility. Finally, plant species turnover throughout the chronosequence was exceptionally high. Few species occurred in every stage of the chronosequence, and none of these belonged to the dominant growth form of woody shrubs.

DIFFERENCES IN BETA DIVERSITY

Beta diversity in the first chronosequence stage was relatively high, presumably due to colonization being initiated with a stochastic subset of the available species. Furthermore, in the absence of a varied and well-established soil seed bank, these stochastic priority effects likely have greater impact on community assembly (e.g. the stochastic community assembly hypothesis, Chase & Leibold 2002; Chase 2010). In the older Quindalup stages (2–3), the decrease in β diversity (both multiplicative and 'true' β diversity) may be the result of priority effects being reduced by stronger competitive displacement due to higher resource availability (e.g. Kardol, Souza & Classen 2013). Alternatively, for some species or functional groups, initial soil development (including the removal of N-limitation) may have promoted more favourable conditions to arise by stage 2 and 3 (e.g. von Gillhaussen *et al.* 2014), thereby favouring a particular community composition and reducing the β diversity in those stages.

In the older, retrogressive stages of the sequence, where the substantial decline in soil nutrients and fertility results in a decrease in productivity (Laliberté *et al.* 2012), most measures of β diversity increased and the species turnover between plots was very high. This does not support a recent hypothesis stating that β diversity should increase with increasing productivity, based on observations of pond and herbaceous communities, albeit of substantially greater fertility (Chase & Leibold 2002; Harrison *et al.* 2006). Indeed, our finding suggests that the interaction of the extremely diverse species pool with nutrient-impoverished soils, together with disturbance, provides the basis for substantial heterogeneity in the community. Significantly, no transition from sampling at a small scale to a large scale was present in our study design – each chronosequence stage covered similar extents – thereby indicating that the change in β diversity was driven by soil, rather than by scale parameters. Since the oldest, most strongly weathered soils all appear to be extremely nutrient impoverished, future studies should determine the abiotic or biotic factors allowing such high β diversity to be maintained at extremely low soil fertility.

EXTREME PLANT SPECIES TURNOVER ACROSS THE CHRONOSEQUENCE

We quantified β diversity using several measures and although they performed rather differently, as could be expected given their different formulations (e.g. see Anderson *et al.* 2011), the agreement in the change between the observed γ diversity and the nonparametric estimators of γ

Table 3. Indicator species (up to the five best, by the indicator statistic) for each single group, and selected combinations of single groups, identified from the multivariate regression tree of Fig. 6

Group(s)	Species	Family	*P(A)*	*P(B)*	Stat	*P*
1	*Lepidosperma calcicola*	Cyperaceae	0.97	0.94	0.96	0.001
	Scaevola thesioides subsp. *thesioides*	Goodeniaceae	1	0.72	0.85	0.012
	Rytidosperma occidentale	Poaceae	0.82	0.72	0.77	0.013
	Podolepis gracilis	Asteraceae	0.91	0.61	0.75	0.018
	Lomandra maritima	Asparagaceae	0.91	0.61	0.74	0.017
2	*Podotheca angustifolia*	Asteraceae	0.52	1	0.72	0.022
	Gastrolobium nervosum	Fabaceae	1	0.50	0.71	0.037
	Melaleuca cardiophylla	Myrtaceae	1	0.50	0.71	0.031
	Ptilotus sp. Northampton	Amaranthaceae	1	0.50	0.71	0.031
	Stylidium junceum	Stylidiaceae	1	0.50	0.71	0.037
3	*Olearia axillaris*	Asteraceae	1	1	1.00	0.001
	Scaevola crassifolia	Goodeniaceae	1	1	1.00	0.001
	Spyridium globulosum	Rhamnaceae	0.97	1	0.99	0.001
	Ficinia nodosa	Cyperaceae	1	0.8	0.89	0.005
	Cassytha aurea	Lauraceae	1	0.7	0.84	0.005
4	*Acacia spathulifolia*	Fabaceae	1	0.67	0.82	0.003
5	*Labichea cassioides*	Fabaceae	0.85	0.71	0.78	0.007
	Hakea costata	Proteaceae	0.89	0.57	0.71	0.006
	Isotropis cuneifolia	Fabaceae	0.82	0.57	0.68	0.023
	Petrophile brevifolia	Proteaceae	0.63	0.71	0.67	0.029
6	*Banksia prionotes*	Proteaceae	1	0.9	0.95	0.001
	Laxmannia sessiliflora subsp. *drummondii*	Asparagaceae	0.97	0.9	0.94	0.002
	Lepidobolus preissianus	Restionaceae	0.84	1	0.91	0.001
	Pileanthus filifolius	Myrtaceae	1	0.7	0.84	0.008
	Corynotheca micrantha	Hemerocallidaceae	0.99	0.7	0.83	0.006
7	*Jacksonia floribunda*	Fabaceae	0.99	0.9	0.94	0.001
	Alexgeorgea nitens	Restionaceae	0.85	1	0.92	0.001
	Conostylis aurea	Haemodoraceae	0.94	0.9	0.92	0.001
	Blancoa canescens	Haemodoraceae	0.91	0.9	0.91	0.001
	Lyginia barbata	Anarthriaceae	1	0.7	0.84	0.003
1, 2	*Acanthocarpus preissii*	Asparagaceae	0.98	0.85	0.91	0.001
	Calandrinia tholiformis	Portulacaceae	1	0.8	0.89	0.001
	Acacia lasiocarpa	Fabaceae	0.82	0.95	0.88	0.001
	Cassytha glabella	Lauraceae	0.98	0.65	0.80	0.011
	Santalum acuminatum	Santalaceae	0.97	0.5	0.70	0.018
4, 5	*Banksia leptophylla* var. *melletica*	Proteaceae	0.94	0.9	0.92	0.001
	Rytidosperma caespitosum	Poaceae	0.94	0.7	0.81	0.006
	Banksia sessilis var. *cygnorum*	Proteaceae	1	0.6	0.77	0.004
	Schoenus grandiflorus	Cyperaceae	0.88	0.50	0.66	0.018
	Lomandra sericea	Asparagaceae	0.87	0.50	0.66	0.020
6, 7	*Amphipogon turbinatus*	Poaceae	1.00	0.90	0.95	0.001
	Banksia attenuata	Proteaceae	1.00	0.70	0.84	0.002
	Hypocalymma xanthopetalum	Myrtaceae	1.00	0.70	0.84	0.003
	Melaleuca leuropoma	Myrtaceae	0.87	0.80	0.83	0.001
	Thysanotus patersonii	Asparagaceae	0.91	0.65	0.77	0.014

P(A) is the probability of the plot being in the group, given the presence of that species in the plot; *P(B)* is the probability of finding that species in a plot within the group; Stat is the indicator statistic ($=\sqrt{P(A) \times P(B)}$); *P* is the *P*-value for the indicator statistic, derived from a permutation test with 1000 permutations.

diversity support the interpretation of increasing β diversity across the chronosequence, as described by the traditional β diversity measures (i.e. multiplicative and additive β diversity). The use of null models of β diversity that assess whether the observed β diversities are higher than would be expected by chance (e.g. Chase *et al.* 2011; Kraft *et al.* 2011) is one approach that has been used to resolve ambiguities arising from differing measures of β diversity. In our study, however, we included a complementary measure of investigating the overall species turnover, namely, assessing the number of shared species between pairs of plots. Turnover increased with chronosequence stage, with higher turnover for woody species than for all growth forms; the general pattern of increasing turnover of species was also evident within each chronosequence stage. Direct comparison of the β diversity of the Jurien Bay chronosequence with other well-studied chronosequences is difficult, because β diversity values have not been reported. However, the commonality of species in several, or all, stages of many chronosequences (e.g. Hawaii, see Crews *et al.* 1995) suggests that, in comparison, this

chronosequence exhibited exceptionally high β diversity and turnover.

In tropical rain forests, soil P gradients in combination with the large regional species pool are thought to promote high β diversity (Kitayama 2012). For example, in central Panama, the species distributions of about 60% of the abundant larger plant species are associated (both positively and negatively) with soil P (Condit *et al.* 2013); the marked soil variation (200-fold variation in resin P) thus contributes to the high regional β diversity. Similarly, β diversity in the Jurien Bay chronosequence seems to be strongly influenced by these factors, as well as by soil pH, despite being unlike tropical rain forests in many respects.

INCREASES AND MAINTENANCE OF ALPHA DIVERSITY

In contrast to the Jurien Bay dune chronosequence, most well-studied chronosequences that contain retrogressive stages are forest-dominated and relatively species poor (e.g. Mark *et al.* 1988; Crews *et al.* 1995; Richardson *et al.* 2004; Wardle *et al.* 2008; Gundale *et al.* 2011). In some of these chronosequences, retrogression is also associated with increases in overall species diversity, leading Wardle *et al.* (2008) to postulate three possibilities for this increase: (1) competition by trees decreases with retrogression; (2) spatial heterogeneity of limiting soil resources increases with declining fertility; (3) competition for light decreases (due to the absence of many large trees), resulting in an increase in light heterogeneity. In this chronosequence, tree species (or woody species, in general) did not decrease in abundance (canopy cover). With the assumption that the canopy cover of trees is a reasonable proxy for their resource use, the first possibility for increasing diversity (decreasing competition for resources by trees) is not supported by the results on the Jurien Bay chronosequence. Competition for light is unlikely to occur in any stage of the Jurien Bay chronosequence, due to the open nature of the canopy in all stages (leaf area index <0.5) and abundant sunshine, typical for a Mediterranean climate. At the level of the subplot, none of the measured soil properties showed any consistent increase in variability; indeed, by using the multivariate dispersion of several key soil variables from the same study plots, Laliberté, Zemunik & Turner (2014) found that within-plot soil spatial heterogeneity did not significantly affect plant species richness. Partitioning of nutrients in different compound forms, however, remains to be quantified in this chronosequence. In particular, partitioning of various organic forms of nutrients (e.g. organic P, Turner 2008) may provide one form of ecologically relevant environmental heterogeneity in the poorest soils of the chronosequence.

At the regional scale, a recent study in the same system showed that the size of the plant species pool in each chronosequence stage is strongly affected by soil pH, with many more calcifuge species present in the species pool in the older, acidic soils (Laliberté, Zemunik & Turner 2014). In addition to environmental filtering by pH, the regional flora contains an unusually large number of species well adapted to P-impoverished soils (Griffin, Hopper & Hopkins 1990; Lambers *et al.* 2014). This suggests that environmental filtering of the regional flora by pH does not remove many species from the species pool in the most P-impoverished soils. This appears to explain the increase in richness observed in the older, P-impoverished stages of the chronosequence (Laliberté, Zemunik & Turner 2014).

Disturbance, long implicated in the maintenance of diversity (Huston 1994; Grime 2001), also likely plays a key role in the maintenance of high diversity along the Jurien Bay chronosequence. The two main disturbances affecting the chronosequence are fire and herbivory. Fire, which in the region has return intervals of between three and 30 years (Department of Conservation and Land Management, 1995, unpublished data), may facilitate seed germination (Dixon, Roche & Pate 1995; Flematti *et al.* 2004). Fire also influences the nutrient status of the soil, potentially setting the ecosystem back to an earlier stage of development due to a temporary increase in soil P availability, and a loss of N through volatilization during burning of surface soil, vegetation and litter (Turner & Laliberté 2015). Herbivory, principally from the western grey kangaroo (*Macropus fuliginosus*), can act to prevent some species from becoming dominant (i.e. it can prevent competitive exclusion). Other factors preventing the establishment of local dominance, for example the Janzen–Connell effect (Janzen 1970; Connell 1971) or negative density dependence mediated by soil-borne pathogens, may also play a role in the maintenance of the high diversity (Laliberté *et al.* 2015), but these remain to be explored further.

SOIL DRIVERS OF THE COMMUNITY COMPOSITION

The climate throughout the chronosequence is virtually the same, and because all plots were located on freely draining sand (i.e. they had broadly similar, sandy soil profiles), climatic and specific soil factors (e.g. flooded conditions) would not confound the effect of the investigated soil chemical properties. Soil N and P concentrations across the chronosequence follow the model proposed by Walker & Syers (1976), with productivity limited by N in the initial stage, N-P co-limitation in intermediate stages and increasingly severe P limitation in the final stages (Laliberté *et al.* 2012; Hayes *et al.* 2014). The shifts in soil P availability, in particular, are far greater than in all other well-studied chronosequences (Skjemstad *et al.* 1992; Crews *et al.* 1995; Richardson *et al.* 2004; Selmants & Hart 2010; Porder & Hilley 2011), with soil total P concentrations declining to some of the lowest ever measured. In this respect, this chronosequence offers valuable insights into community compositional change as soils become strongly nutrient impoverished; many other well-studied chronosequences have initial stages with far higher soil P concentrations, so the insights garnered from those systems on richer substrates are complemented to some degree by this chronosequence.

The key soil variables explaining the similarities of plots, as produced from the canonical redundancy analysis, were pH

and (dissolved organic) N, as well as the macronutrients, K and Mg, and the micronutrient Fe. We expected that soil P availability would be a key explanatory soil variable, but this was masked by its strong correlation with soil pH, as observed along other chronosequences (e.g. Richardson *et al.* 2004). Indeed, pH plays a critical role in shaping α diversity by filtering out species from the regional species pool (Laliberté, Zemunik & Turner 2014). Nonetheless, the strong role of soil N and P (and pH) broadly support the hypothesis of community change with pedogenic shifts from N to P limitation of plant productivity (Peltzer *et al.* 2010). With respect to the micronutrient explanatory variable Fe, the lack of any observable micronutrient deficiencies in the plants suggests that it most likely reflects correlations of soil properties (iron oxide coatings on sand grains, Turner & Laliberté 2015) rather than being a causal agent in its own right. The fact that plant species can survive for successive generations in soils severely impoverished in micronutrients, which is especially evident in the older chronosequence stages, is likely a consequence of their ability to take up P via its mobilization by root exudates (Lambers *et al.* 2006); a side effect of the P mobilization would be the uptake of various micronutrients (Muler *et al.* 2014). For example, the uptake of manganese, which is then concentrated in the foliage, appears to be highly indicative of carboxylate release for mobilizing sorbed P (Lambers *et al.* 2015).

DOMINANT PLANT FAMILIES

The Fabaceae were the only plant family with substantial canopy cover throughout all stages of the chronosequence. Most of these leguminous plants were potentially N-fixing, and those that were N-fixing did have substantial cover in the first, N-limited stage of the sequence; however, their cover was not significantly greater than in several other stages. Nevertheless, the overall abundance of N-fixing plants throughout the chronosequence may assist with the acquisition of organic P from the soil using phosphatases (e.g. Houlton *et al.* 2008), as organic P becomes a large proportion of total P in the older, P-impoverished soils (Turner & Laliberté 2015). In the youngest (N-limited) soils, plants lacking the ability to fix N were nonetheless often found in abundance in subplots without any co-occurring N-fixing plants, thus potentially indicating another source of N (e.g. via heterotrophic soil bacteria or cyanobacterial mats on the soil surface, which occur during the winter on the youngest soils). Further research is warranted to identify other significant N sources.

Several species from the dominant families Fabaceae and Myrtaceae were found in many stages of the chronosequence, with two species, a small tree, *Acacia rostellifera* (Fabaceae), and a shrub, *Melaleuca systena* (Myrtaceae), occurring in all but the Bassendean stage (6). Both species form dual mycorrhizal associations (with arbuscular and ectomycorrhizal fungi), with *A. rostellifera* additionally having the capacity to fix atmospheric N. Given the wide range of soil nutrients over which these species occur, variation in the degree or type of mycorrhization could be expected (Lambers *et al.* 2008; Zemunik *et al.* 2015), and these species may serve as valuable models for exploring intraspecific changes in plant functioning across a broad soil fertility gradient. Other families, such as the Myrtaceae and Dilleniaceae, were also key in many of the stages, whilst the Proteaceae were dominant in the final three stages, where soil pH and soil P availability were lowest.

CONCLUDING REMARKS

The extreme gradient in P availability and pH across this chronosequence terminates in extremely P-depleted soils, likely representing the lower limit of soil P concentrations globally. By extending the range of documented responses of successional plant communities to diminishing soil fertility, the Jurien Bay chronosequence provides an invaluable contribution to the understanding of ecosystem progression and retrogression. Our finding of increasing α and β diversity and extremely high species turnover with long-term soil development points to a novel mechanism whereby extremely low soil fertility, rather than high productivity, promotes β diversity. In conclusion, our results further highlight the strong linkages between plant community assembly and soil development.

Acknowledgements

G.Z. acknowledges the assistance of many helpers and volunteers in conducting the flora surveys. G.Z. was supported by a scholarship from the Paul Hasluck Bequest administered by the Kwongan Foundation. Field sampling and soil analyses were funded by a DECRA (DE120100352) from the Australian Research Council and research grants from The University of Western Australia to E.L. and by an ARC Discovery (DP0985685) to H.L. We acknowledge the Department of Parks and Wildlife (Western Australia) and the Shires of Dandaragan and Coorow for permission to conduct research on land under their administration.

Data accessibility

The data sets used in the analyses of this study are placed in the Aekos repository, http://aekos.org.au/home, DOI 10.4227/05/56AEB32FC11D4.

References

Anderson, M.J. (2006) Distance-based tests for homogeneity of multivariate dispersions. *Biometrics*, **62**, 245–253.

Anderson, M.J., Crist, T.O., Chase, J.M., Vellend, M., Inouye, B.D., Freestone, A.L., Sanders, N.J., Cornell, H.V., Comita, L.S. & Davies, K.F. (2011) Navigating the multiple meanings of β diversity: a roadmap for the practicing ecologist. *Ecology Letters*, **14**, 19–28.

Borcard, D., Gillet, F. & Legendre, P. (2011) *Numerical Ecology with R*. Springer, New York, NY, USA.

Chao, A. (1984) Nonparametric estimation of the number of classes in a population. *Scandinavian Journal of Statistics*, **11**, 265–270.

Chase, J.M. (2010) Stochastic community assembly causes higher biodiversity in more productive environments. *Science*, **328**, 1388–1391.

Chase, J.M. & Leibold, M.A. (2002) Spatial scale dictates the productivity–biodiversity relationship. *Nature*, **416**, 427–430.

Chase, J.M., Kraft, N.J., Smith, K.G., Vellend, M. & Inouye, B.D. (2011) Using null models to disentangle variation in community dissimilarity from variation in α-diversity. *Ecosphere*, **2**, Article 24.

Chiarucci, A., Enright, N.J., Perry, G.L.W., Miller, B.P. & Lamont, B.B. (2003) Performance of nonparametric species richness estimators in a high diversity plant community. *Diversity and Distributions*, **9**, 283–295.

Colwell, R.K. (2013) EstimateS: Statistical estimation of species richness and shared species from samples. Version 9. http://purl.oclc.org/estimates.

Condit, R., Engelbrecht, B.M., Pino, D., Pérez, R. & Turner, B.L. (2013) Species distributions in response to individual soil nutrients and seasonal drought across a community of tropical trees. *Proceedings of the National Academy of Sciences of the United States of America*, **110**, 5064–5068.

Connell, J.H. (1971) On the role of natural enemies in preventing competitive exclusion in some marine animals and in rain forest trees. *Dynamics of Populations*, **298**, 312.

Connell, J.H. & Slatyer, R.O. (1977) Mechanisms of succession in natural communities and their role in community stability and organization. *The American Naturalist*, **111**, 1119.

Cowling, R.M., Rundel, P.W., Lamont, B.B., Arroyo, M.K. & Arianoutsou, M. (1996) Plant diversity in Mediterranean-climate regions. *Trends in Ecology & Evolution*, **11**, 362–366.

Crews, T.E., Kitayama, K., Fownes, J.H., Riley, R.H., Herbert, D.A., Mueller-Dombois, D. & Vitousek, P.M. (1995) Changes in soil phosphorus fractions and ecosystem dynamics across a long chronosequence in Hawaii. *Ecology*, **76**, 1407–1424.

De Cáceres, M. & Legendre, P. (2009) Associations between species and groups of sites: indices and statistical inference. *Ecology*, **90**, 3566–3574.

De Cáceres, M., Legendre, P. & Moretti, M. (2010) Improving indicator species analysis by combining groups of sites. *Oikos*, **119**, 1674–1684.

De'ath, G. (2002) Multivariate regression trees: a new technique for modeling species-environment relationships. *Ecology*, **83**, 1105–1117.

De'ath, G. (2014) mvpart: Multivariate partitioning. R package version 1.6-2. http://CRAN.R-project.org/package=mvpart.

Department of Conservation and Land Management (1995) Management Plan: Lesueur National Park and Coomallo Nature Reserve 1995–2005.

Dixon, K.W., Roche, S. & Pate, J.S. (1995) The promotive effect of smoke derived from burnt native vegetation on seed germination of Western Australian plants. *Oecologia*, **101**, 185–192.

Dray, S., Legendre, P. & Blanchet, G. (2013) packfor: Forward Selection with permutation (Canoco p.46). *R package version 0.0-8/r109*. http://R-Forge.R-project.org/projects/sedar/.

Flematti, G.R., Ghisalberti, E.L., Dixon, K.W. & Trengove, R.D. (2004) A compound from smoke that promotes seed germination. *Science*, **305**, 977.

von Gillhaussen, P., Rascher, U., Jablonowski, N.D., Plückers, C., Beierkuhnlein, C. & Temperton, V.M. (2014) Priority effects of time of arrival of plant functional groups override sowing interval or density effects: a grassland experiment. *PLoS One*, **9**, e86906.

Griffin, E.A., Hopper, S.D. & Hopkins, A.J.M. (1990) Flora. *Nature Conservation, Landscape and Recreation values of the Lesueur area* (eds A.A. Burbidge, S.D. Hopper & S. van Leeuwin), pp. 39–70. Environmental Protection Authority, Perth, Australia.

Grime, J.P. (2001) *Plant Strategies, Vegetation Processes, and Ecosystem Properties*. John Wiley & Sons, Chichester, UK.

Gundale, M.J., Fajardo, A., Lucas, R.W., Nilsson, M.-C. & Wardle, D.A. (2011) Resource heterogeneity does not explain the diversity-productivity relationship across a boreal island fertility gradient. *Ecography*, **34**, 887–896.

Harrison, S., Davies, K.F., Safford, H.D. & Viers, J.H. (2006) Beta diversity and the scale-dependence of the productivity-diversity relationship: a test in the Californian serpentine flora. *Journal of Ecology*, **94**, 110–117.

Hayes, P., Turner, B.L., Lambers, H. & Laliberté, E. (2014) Foliar nutrient concentrations and resorption efficiency in plants of contrasting nutrient-acquisition strategies along a 2-million-year dune chronosequence. *Journal of Ecology*, **102**, 396–410.

Holm, S. (1979) A simple sequentially rejective multiple test procedure. *Scandinavian Journal of Statistics*, **6**, 65–70.

Hopper, S.D. & Gioia, P. (2004) The southwest Australian floristic region: evolution and conservation of a global hot spot of biodiversity. *Annual Review of Ecology, Evolution, and Systematics*, **35**, 623–650.

Houlton, B.Z., Wang, Y.-P., Vitousek, P.M. & Field, C.B. (2008) A unifying framework for dinitrogen fixation in the terrestrial biosphere. *Nature*, **454**, 327–330.

Huston, M.A. (1994) *Biological Diversity: The Coexistence of Species*. Cambridge University Press, Cambridge, UK.

Janzen, D.H. (1970) Herbivores and the number of tree species in tropical forests. *American Naturalist*, **104**, 501–528.

Jenny, H. (1946) Arrangement of soil series and types according to functions of soil-forming factors. *Soil Science*, **61**, 375–392.

Kardol, P., Souza, L. & Classen, A.T. (2013) Resource availability mediates the importance of priority effects in plant community assembly and ecosystem function. *Oikos*, **122**, 84–94.

Kitayama, K. (2012) Beta diversity of tree species along soil-P gradients in tropical montane rain forests of contrasting species pools: does biodiversity matter in stabilizing forest ecosystems? *Pacific Science*, **66**, 151–160.

Kraft, N.J., Comita, L.S., Chase, J.M., Sanders, N.J., Swenson, N.G., Crist, T.O., Stegen, J.C., Vellend, M., Boyle, B. & Anderson, M.J. (2011) Disentangling the drivers of β diversity along latitudinal and elevational gradients. *Science*, **333**, 1755–1758.

Laliberté, E., Zemunik, G. & Turner, B.L. (2014) Environmental filtering explains variation in plant diversity along resource gradients. *Science*, **345**, 1602–1605.

Laliberté, E., Turner, B.L., Costes, T., Pearse, S.J., Wyrwoll, K.H., Zemunik, G. & Lambers, H. (2012) Experimental assessment of nutrient limitation along a 2-million-year dune chronosequence in the south-western Australia biodiversity hotspot. *Journal of Ecology*, **100**, 631–642.

Laliberté, E., Grace, J.B., Huston, M.A., Lambers, H., Teste, F.P., Turner, B.L. & Wardle, D.A. (2013) How does pedogenesis drive plant diversity? *Trends in Ecology & Evolution*, **28**, 331–340.

Laliberté, E., Lambers, H., Burgess, T.I. & Wright, S.J. (2015) Phosphorus limitation, soil-borne pathogens and the coexistence of plant species in hyperdiverse forests and shrublands. *New Phytologist*, **206**, 507–521.

Lambers, H., Shane, M.W., Cramer, M.D., Pearse, S.J. & Veneklaas, E.J. (2006) Root structure and functioning for efficient acquisition of phosphorus: matching morphological and physiological traits. *Annals of Botany*, **98**, 693–713.

Lambers, H., Raven, J.A., Shaver, G.R. & Smith, S.E. (2008) Plant nutrient-acquisition strategies change with soil age. *Trends in Ecology & Evolution*, **23**, 95–103.

Lambers, H., Shane, M.W., Laliberté, E., Swarts, N.D., Teste, F. & Zemunik, G. (2014) Plant mineral nutrition. *Plant Life on the Sandplains in Southwest Australia, a Global Biodiversity Hotspot* (ed. H. Lambers), pp. 101–127. UWA Publishing, Crawley.

Lambers, H., Hayes, P.E., Laliberté, E., Oliveira, R.S. & Turner, B.L. (2015) Leaf manganese accumulation and phosphorus-acquisition efficiency. *Trends in Plant Science*, **20**, 83–90.

Legendre, P. & Gallagher, E.D. (2001) Ecologically meaningful transformations for ordination of species data. *Oecologia*, **129**, 271–280.

Lenth, R.V. (2014) lsmeans: Least-Squares Means. R package version 2.00-4. http://CRAN.R-project.org/package=lsmeans.

Mark, A., Grealish, G., Ward, C. & Wilson, J. (1988) Ecological studies of a marine terrace sequence in the Waitutu Ecological District of southern New Zealand. Part 1: the vegetation and soil patterns. *Journal of the Royal Society of New Zealand*, **18**, 29–58.

Martínez-García, L.B., Richardson, S.J., Tylianakis, J.M., Peltzer, D.A. & Dickie, I.A. (2015) Host identity is a dominant driver of mycorrhizal fungal community composition during ecosystem development. *New Phytologist*, **205**, 1565–1576.

McArthur, W.M. (2004) *Reference Soils of South-Western Australia*. Department of Agriculture, Perth, Australia.

Mehlich, A. (1984) Mehlich 3 soil test extractant: A modification of Mehlich 2 extractant. *Communications in Soil Science & Plant Analysis*, **15**, 1409–1416.

Muler, A., Oliveira, R., Lambers, H. & Veneklaas, E. (2014) Does cluster-root activity benefit nutrient uptake and growth of co-existing species? *Oecologia*, **174**, 23–31.

Myers, N., Mittermeier, R.A., Mittermeier, C.G., Da Fonseca, G.A. & Kent, J. (2000) Biodiversity hotspots for conservation priorities. *Nature*, **403**, 853–858.

Odum, E.P. (1969) The strategy of ecosystem development. *Science*, **164**, 262–270.

Oksanen, J., Blanchet, F.G., Kindt, R., Legendre, P., Minchin, P.R., O'Hara, R.B., Simpson, G.L., Solymos, P., Stevens, M.H.H. & Wagner, H. (2013) vegan: Community Ecology Package. R package version 2.0-9. http://CRAN.R-project.org/package=vegan.

Peltzer, D.A., Wardle, D.A., Allison, V.J., Baisden, W.T., Bardgett, R.D., Chadwick, O.A. *et al.* (2010) Understanding ecosystem retrogression. *Ecological Monographs*, **80**, 509–529.

Pinheiro, J., Bates, D., DebRoy, S., Sarkar, D. & Team, R.D.C. (2015) nlme: Linear and Nonlinear Mixed Effects Models. R package version 3.1-120.

Porder, S. & Hilley, G.E. (2011) Linking chronosequences with the rest of the world: predicting soil phosphorus content in denuding landscapes. *Biogeochemistry*, **102**, 153–166.

Quantum GIS Development Team (2012) *Quantum GIS*. Geographic Information System. http://qgis.org.

R Development Core Team (2013) *R: A Language and Environment for Statistical Computing*. R Foundation for Statistical Computing, Vienna, Austria.

Richardson, S.J., Peltzer, D.A., Allen, R.B., McGlone, M.S. & Parfitt, R.L. (2004) Rapid development of phosphorus limitation in temperate rainforest along the Franz Josef soil chronosequence. *Oecologia*, **139**, 267–276.
Selmants, P.C. & Hart, S.C. (2010) Phosphorus and soil development: does the Walker and Syers model apply to semiarid ecosystems? *Ecology*, **91**, 474–484.
Skjemstad, J., Fitzpatrick, R.W., Zarcinas, B. & Thompson, C. (1992) Genesis of podzols on coastal dunes in southern Queensland. II. Geochemistry and forms of elements as deduced from various soil extraction procedures. *Soil Research*, **30**, 615–644.
Stevens, P.R. & Walker, T.W. (1970) The chronosequence concept and soil formation. *The Quarterly Review of Biology*, **45**, 333.
Thompson, C.H. (1981) Podzol chronosequences Queensland. *Nature*, **291**, 59–61.
Tuomisto, H. (2010) A diversity of beta diversities: straightening up a concept gone awry. Part 1. Defining beta diversity as a function of alpha and gamma diversity. *Ecography*, **33**, 2–22.
Turner, B.L. (2008) Resource partitioning for soil phosphorus: a hypothesis. *Journal of Ecology*, **96**, 698–702.
Turner, B.L. & Laliberté, E. (2015) Soil development and nutrient availability along a 2 million-year coastal dune chronosequence under species-rich Mediterranean shrubland in southwestern Australia. *Ecosystems*, **18**, 287–309.
Vitousek, P.M. (2004) *Nutrient Cycling and Limitation: Hawai'i as a Model System*. Princeton University Press, Princeton, NJ, USA.
de Vries, A. & Ripley, B.D. (2013) ggdendro: Tools for extracting dendrogram and tree diagram plot data for use with ggplot. R package version 0.1-14. http://CRAN.R-project.org/package=ggdendro.
Walker, T.W. & Syers, J.K. (1976) The fate of phosphorus during pedogenesis. *Geoderma*, **15**, 1–19.
Walker, L.R., Wardle, D.A., Bardgett, R.D. & Clarkson, B.D. (2010) The use of chronosequences in studies of ecological succession and soil development. *Journal of Ecology*, **98**, 725–736.
Wardle, D.A., Bardgett, R.D., Walker, L.R., Peltzer, D.A. & Lagerström, A. (2008) The response of plant diversity to ecosystem retrogression: evidence from contrasting long-term chronosequences. *Oikos*, **117**, 93–103.
Zemunik, G., Turner, B.L., Lambers, H. & Laliberté, E. (2015) Diversity of plant nutrient-acquisition strategies increases during long-term ecosystem development. *Nature Plants*, **1**, 1–4.

Received 15 April 2015; accepted 20 January 2016
Handling Editor: Andy Dyer

Supporting Information

Additional Supporting Information may be found in the online version of this article:

Figure S1. Study plots and the dune systems of the Jurien Bay dune chronosequence.

Figure S2. Photographs of representative examples of plots throughout the dune chronosequence.

Figure S3. Mean densities of plants for all, perennial and woody growth forms.

Figure S4. Non-metric multidimensional scaling plot for woody plant species.

Figure S5. Canonical redundancy analysis of the plant species abundance data.

Figure S6. Multivariate regression tree giving site groupings based on soil variables.

Figure S7. Mean relative cover of the eight most dominant families in each chronosequence stage.

Figure S8. Mean relative cover of the plant growth forms in each chronosequence stage.

Figure S9. Mean canopy height, absolute cover and bare cover for plants rooted in the plots within each stage of the chronosequence.

Figure S10. Variation of the standard deviation of the soil variables measured in each plot.

Table S1. Plot codes and coordinates for all plots in the Jurien Bay dune chronosequence.

Table S2. The most abundant species in the Jurien Bay dune chronosequence.

Table S3. The number of plant taxa within each of the classified growth forms found in the chronosequence.

Table S4. Mean species richness of the most abundant families, by cover, in the chronosequence.

Table S5. Permuted *F*-statistics and the associated *P*-values for the beta (β) dispersions of plots grouped by chronosequence stage, considering either all species or woody species only.